An Adaptive Approach to Reducing Registration Noise Effects in Unsupervised Change Detection

Lorenzo Bruzzone, *Senior Member, IEEE*, and Roberto Cossu, *Student Member, IEEE*

***Abstract*—In this paper, an approach to reducing the effects of registration noise in unsupervised change detection is proposed. The approach is formulated in the framework of the change vector analysis (CVA) technique. It is composed of two main phases. The first phase aims at estimating in an adaptive way (given the specific pair of images considered) the registration-noise distribution in the magnitude-direction domain of the difference vectors. The second phase exploits the estimated distribution to define an effective decision strategy to be applied to the difference image. Such a strategy allows one to perform change detection by significantly reducing the effects of registration noise. Experimental results obtained on simulated and real multitemporal datasets confirm the effectiveness of the proposed approach.**

***Index Terms*—Change detection, change vector analysis, image registration, multitemporal images, nonparametric adaptive estimation, registration noise, remote sensing, unsupervised techniques.**

I. Introduction

THE GROWING interest in environmental monitoring, in particular, in detecting changes that have occurred on the earth's surface, makes it crucial to develop effective unsupervised change-detection techniques for the analysis of multitemporal remote sensing images [1]–[4]. However, a major problem in the development of such unsupervised techniques is that several sources of noise may significantly affect the change-detection process. Among these sources of noise, it is worth mentioning those dependent on different conditions at the two considered acquisition times, like atmospheric differences, differences in vegetational phenology, differences in the shadows present in the images, etc. [1], [5]. For these reasons, the development of effective automatic unsupervised change-detection techniques is a challenging task.

The most widely used unsupervised change-detection techniques involve a pixel-by-pixel comparison of two multispectral remote sensing images acquired at the same area at different times [1]–[3]. Consequently, in order to perform change detection accurately, it is mandatory to apply a preliminary coregistration process to multitemporal images so that pixels in the same positions on the two images correspond to the same area on the ground. Many papers have been published in the literature concerning the development of registration algorithms for multitemporal and/or multisensor remote sensing images [6]–[8]. However, although complex registration procedures have been devised, generally, in remote sensing applications, it is not possible to obtain a perfect alignment of multitemporal images. This mainly depends on the fact that the presence of local defects in the geometries of the acquired images (e.g., due to irregular movements of the acquisition platform) does not allow one to achieve a perfect alignment, even by applying sophisticated geometrical transformations to the images. Consequently, when multitemporal images are compared, the residual misregistration results in an additional and very critical source of noise, which is called "registration noise" [5], [9]. Generally, it is difficult to reduce the effects of registration noise because they depend on several significant factors (e.g., the stability of the acquisition platform, the structure of the considered scene, the spatial resolution of the sensor used, etc.). This prevents one from formulating an analytical model of this noise and, consequently, from defining effective processing algorithms.

Even though in the literature special attention has been given to the development of advanced registration techniques [6]–[8], less attention has been devoted to devising approaches aimed at reducing the effects of the residual misalignment in the change-detection process. In [10], the capabilities of two heuristic approaches to reducing registration-noise effects are compared. In particular, an image smoothing technique and an adaptive filtering method are presented. In [11], a change-detection algorithm robust to registration noise is proposed that allows the detection of land-cover changes by exploiting the information available in multispectral remote sensing images. Such an algorithm uses the spectral bands where investigated changes are not visible in order to identify the effects of registration noise on the specific scene analyzed and to reduce them in spectral channels where changes can be detected. In [12] and [13], a modeling approach is introduced that assumes that misregistration effects are locally uniform and can be estimated and compensated for by analyzing the spatial brightness gradients. Although all the above approaches may be effective under different operating conditions, they are based on empirical observations or on general image-processing methods. A major theoretical issue that limits the development of effective change-detection approaches robust to registration noise is the lack of suitable models (or analysis procedures) capable of accurately describing the distribution of this noise.

In this paper, we focus our attention on the problem of reducing registration noise in change detection, and address the aforementioned issue with an adaptive unsupervised technique. Due to the complexity of representing the registration noise by using a general model, we propose to estimate it adaptively in each specific scene to be analyzed; to this end, we suggest

Manuscript received October 30, 2002; revised May 13, 2003. This work was supported by the Italian Ministry of University and Scientific and Technological Research (MIUR).

The authors are with the Department of Information and Communication Technology, University of Trento, I-38050 Trento, Italy (e-mail: lorenzo.bruzzone@ing.unitn.it).

Digital Object Identifier 10.1109/TGRS.2003.817268

0196-2892/03$17.00 © 2003 IEEE

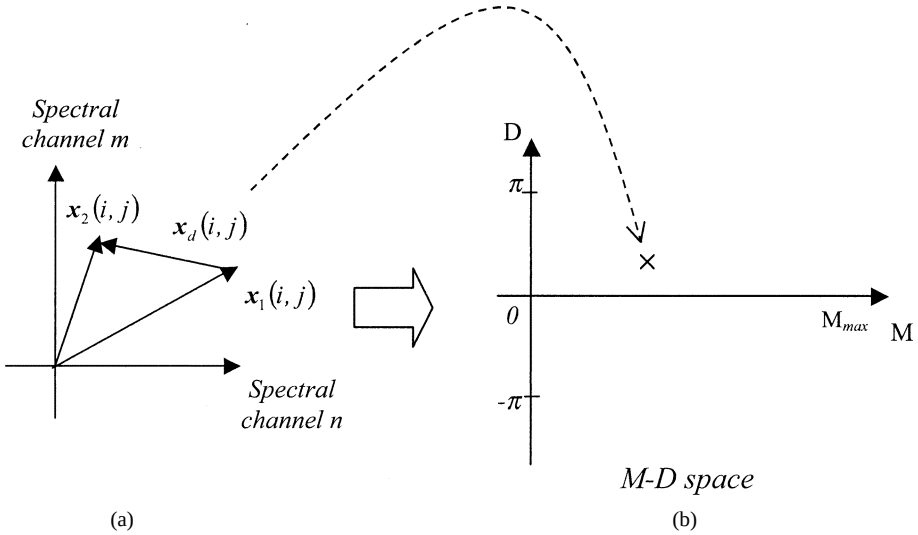

Fig. 1. Schematic representation of the difference vector associated with the pixel $x(i,j)$. (a) Space of the original spectral channels. (b) Magnitude–Direction (M–D) space.

adopting a nonparametric approach. Then, the estimated registration-noise distribution is used to define an effective local decision strategy to produce an accurate change-detection map. Experiments carried out on both a simulated and a real dataset confirm the effectiveness of the presented method.

The paper is organized into six sections. Section II deals with the problem formulation. Section III describes the proposed adaptive approach to reducing registration-noise effects. Section IV presents a simple but effective strategy capable of exploiting contextual information in the process of generating the change-detection map. Experimental results are reported in Section V. Finally, in Section VI, a discussion is provided and conclusions are drawn.

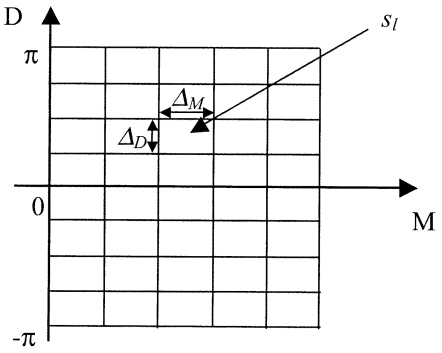

Fig. 2. Representation of the quantized M–D space. The quantization has been carried out in a uniform way into cells of size $\Delta_M \times \Delta_D$.

II. Problem Formulation

Let $\mathbf{X}_1$ and $\mathbf{X}_2$ be two multispectral remote sensing images (of size $W \times H$) acquired at the same geographical area at two different times. Let $x(i,j)$ represent a generic pixel with position coordinates (i,j). Let $\boldsymbol{x}_1(i,j)$ and $\boldsymbol{x}_2(i,j)$ denote the feature vectors associated with the pixel $x(i,j)$ in $\mathbf{X}_1$ and $\mathbf{X}_2$, respectively. We assume that the two images have been coregistered by using standard techniques in order to minimize the mean square error computed on a set of ground control points (GCPs) [1], [14], [15]. We also assume that a residual misregistration between the two images is present (this is a typical situation in remote sensing problems). The objective of the proposed approach is to perform unsupervised change detection by reducing as much as possible the errors due to the residual misregistration.

In the development of the approach, we make the assumption that the residual registration noise can be modeled as a translational effect between the two analyzed images. This represents a simplification, as compared with some real cases in which rotational and scaling effects may be present (especially if images acquired from different angles of view or by different sensors are considered). However, this assumption is reasonable if the analysis concerns image subwindows whose sizes are chosen such that the rotational and scaling effects of registration can be neglected as respect to translational effects. Unfortunately, it is not possible to define *a priori* such sizes as they depend on the images considered; consequently, they should be specifically evaluated on the particular pair of images to be analyzed. It is worth noting that the aim of our approach is to characterize the registration noise from a statistical point of view as, even in the case of small subwindows of the entire images, it is not realistic to assume a perfect uniformity of the properties of the residual misalignment.

The proposed approach is presented in the framework of the well-known and widely used change vector analysis (CVA) technique [1]–[3]. This technique performs change detection by differencing the feature vectors of pixels with the same spatial coordinates in the two considered images. Let $\mathbf{X}_d$ represent the difference image obtained by applying the CVA to the images $\mathbf{X}_1$ and $\mathbf{X}_2$. Let $\boldsymbol{x}_d(i,j)$ denote the spectral change vector associated with the pixel $x(i,j)$ in the difference image, i.e.,

$$\boldsymbol{x}_d(i,j) = \boldsymbol{x}_2(i,j) - \boldsymbol{x}_1(i,j). \tag{1}$$

Let $x_d^{\text{mag}}(i,j)$ denote the magnitude of the difference vector $\boldsymbol{x}_d(i,j)$. It follows that unchanged pixels show small gray-level values in the magnitude of the difference vector, whereas changed pixels present rather large values. Consequently, the change-detection map is obtained by thresholding the value

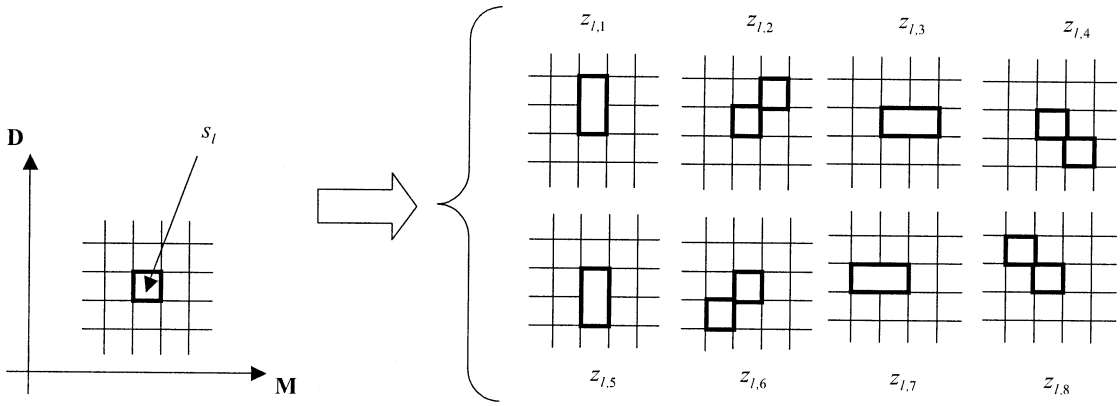

Fig. 3. Schematic representation of the different macrocells $z_{l,h} \in Z_l$ $(h = 1, \ldots, 8)$ associated with the cell s_l in the M–D space when the contextual strategy is adopted. The macrocells are considered in order to exploit the contextual information in the aforesaid space.

$x_d^{\mathrm{mag}}(i,j)$ according to a predefined threshold ν_{th}. In some applications, the direction of the difference vector $\boldsymbol{x}_d(i,j)$ is also exploited to discriminate among different kinds of changes.

For simplicity, we present the proposed method under the assumption that the CVA technique is applied to only two spectral channels of the considered multispectral images. This results in difference vectors that have only two components. Consequently, each vector can be represented in a two-dimensional (2-D) space described by its magnitude and an angle (ranging from $-\pi$ to $+\pi$) that indicates its direction (we call this space "M–D space") (see Fig. 1). If more spectral channels are used, a higher dimensional space must be defined, since the directions of the difference vectors then require more angular coordinates to be represented. However, it is straightforward to extend the proposed method to a higher dimensional case.

III. Proposed Approach Robust to Registration Noise

The proposed approach is composed of two phases. In the first phase, the distribution of registration noise in the M–D space is estimated for the specific scene of interest considered. In the second phase, the estimated distribution is used to define a local adaptive decision strategy for carrying out change detection in accordance with the registration-noise distribution.

In the following, both phases are described in greater detail.

A. Adaptive and Nonparametric Estimation of the Distribution of Registration Noise in the M–D Space

This first phase aims to perform a nonparametric estimation of the registration-noise distribution in the M–D space. For this purpose, a single-date image (e.g., let us choose $\mathbf{X}_1$) of the considered multitemporal dataset is artificially misregistered to itself in several different ways. In particular, a set $\boldsymbol{\Gamma} = \{\mathbf{X}_1^i\}(i = 1, \ldots, M)$ of M misregistered images $\mathbf{X}_1^i$ is generated for different misregistration values in the horizontal and vertical directions. Let $\Phi = \{(x_p, y_q)\}$ (with x_p ranging from $-x_{\max}$ to $+x_{\max}$ and y_q ranging from $-y_{\max}$ to $+y_{\max}$, both by a predefined step) be the set of M misregistration values chosen to misregister $\mathbf{X}_1$. In order to consider values of x_p and y_q equal to fractions of pixels, the image $\mathbf{X}_1$ is oversampled by using the discrete Fourier transform (DFT). After the shifting obtained by working in the Fourier domain, the image is resampled in order to resize it according to its original dimensions.

The CVA technique is applied to the original and misregistered images (i.e., $\mathbf{X}_1$ and $\mathbf{X}_1^i$, with $i = 1, \ldots, M$), and the distributions of the resulting difference vectors in the M–D space are analyzed. It is worth noting that the values of the magnitudes of the difference vectors depend on the dynamics of the images $\mathbf{X}_1$ and $\mathbf{X}_1^i$, whereas the angles describing the directions of such vectors range from $-\pi$ to π. The analysis is carried out by quantizing the M–D space into $N \times L$ uniform cells of size $\Delta_M \times \Delta_D$ (see Fig. 2). Let $S = \{s_1, \ldots, s_{N \times L}\}$ be the set of cells obtained by the quantization process, and let $g_l(x_p, y_q)$ be the number of pixels contained in the cell s_l when the difference vectors are generated for a shift (i.e., misregistration) of $(x_p, y_q) \in \Phi$ pixels. In this situation, the distribution of the difference vectors in the M–D space depends only on the registration noise (as we are comparing an image with a misregistered copy of itself). It is worth noting that if $(x_p, y_q) = (0, 0)$, then all the pixels are located in the origin of the 2-D M–D space. On the basis of the value $g_l(x_p, y_q)$, an estimate of the probability $P_l(n/x_p, y_q)$ of having a pixel affected by registration noise in the cell s_l, given the misregistration of (x_p, y_q) pixels, can be obtained by the following equation:

$$P_l(n/x_p, y_q) = \frac{g_l(x_p, y_q)}{W \times H} = \frac{g_l(x_p, y_q)}{\sum_{j=1}^{N \times L} g_j(x_p, y_q)}. \qquad (2)$$

This probability can be estimated for all the $N \times L$ quantization cells considered and for all the misregistration values $(x_p, y_q) \in \Phi$ selected. Then, from such probabilities, different strategies can be derived to approximate the global probability $P_l(n)$ of having pixels affected by registration noise in the quantization cell s_l $(l = 1, \ldots, N \times L)$ and, hence, the global density $p(n)$ of the distribution of registration noise in the M–D space. In the following, we propose three different strategies: 1) the mean-based strategy; 2) the maximum-based strategy; 3) the correlation-based strategy.

1) Mean-Based Strategy: The mean-based strategy models the local registration-noise distribution in the M–D space on the basis of a global analysis of $P_l(n/x_p, y_q)$ obtained for all the misregistration values $(x_p, y_q) \in \Phi$ considered. In particular,

(a) (b) (c)

Fig. 4. Simulated dataset utilized in the experiments. (a) Spectral channel 3 of the image $\mathbf{X}_1$. (b) Spectral channel 3 of the image $\mathbf{X}_2$ obtained by inserting simulated changes in $\mathbf{X}_1$. (c) Map of the areas with simulated changes.

TABLE I
CHANGE-DETECTION RESULTS PROVIDED BY THE STANDARD CVA TECHNIQUE ON THE DIFFERENT SIMULATED DATASETS CONSIDERED

Misalignment between the simulated multitemporal images	Change-detection errors (# pixels)		
	Missed alarms	False alarms	Total error
(2,2)	178	632	810
(1,2)	249	521	770
(1.5,1.5)	188	514	702
(0.5,1.5)	178	503	610
(1,1)	282	332	614

the rationale for this strategy consists in modeling the registration noise in each quantization cell with the mean of the noise resulting from the pairs of misregistration values considered in the set Φ. Consequently, this strategy estimates the registration noise in each cell s_l via the following equation:

$$\hat{P}_l(n) = \frac{1}{M} \sum_{(x_p, y_q) \in \Phi} P_l(n/x_p, y_q). \tag{3}$$

This simple strategy exhibits the drawback of modeling the average effects of the registration noise in the M–D space without considering the actual direction of the residual misalignment. As a consequence, it may result in a raw estimate of the registration-noise effects.

2) Maximum-Based Strategy: This strategy is similar to the previous one, except for the average operator, which is replaced with the maximum operator. In particular, the rationale for this strategy consists in modeling the registration noise in each quantization cell with the maximum possible noise resulting from the pairs of misregistration values considered in the set Φ, i.e., with the noisiest situation that may occur in each cell as a consequence of the residual misalignment

$$\hat{P}_l(n) = \max_{(x_p, y_q) \in \Phi} \{P_l(n/x_p, y_q)\}. \tag{4}$$

As is the case with the mean-based strategy, this technique has the drawback of modeling the effects of the registration noise in the M–D space without trying to identify the actual average direction of the residual misalignment. However, the maximum-based strategy assumes the noisiest situation for each cell. As a consequence, this strategy may involve an overestimate of the actual registration-noise effects.

3) Correlation-Based Strategy: Unlike the previous two strategies, the correlation-based technique aims at estimating the pair of misregistration values (x_p^*, y_q^*) that are statistically best suited to characterizing the considered subwindow of the analyzed multitemporal images (the terms "statistically best suited" is used to recall that it is not realistic to assume the same misregistration value for all the pixels of a subwindow). Then this strategy carries out the estimation of the registration-noise distribution on the basis of such values. A possible approach to estimating the value of misregistration lies in evaluating the residual misregistration computed at the GCPs that fall into the considered subwindow after the registration phase. However, it is well known that this estimate is usually inaccurate, and does not represent the real situation in the whole subwindow of the image considered. For this reason, we propose an alternative method that consists in comparing (in the M–D space) the difference-vector distributions in the considered multitemporal images with the distributions of the difference vectors obtained by applying the CVA technique to the images $\mathbf{X}_1$ and $\mathbf{X}_1^i$ (with $i = 1, \ldots, M$). (It is worth stressing that the difference vectors obtained by applying the CVA technique to the images $\mathbf{X}_1$ and $\mathbf{X}_1^i$ represent the registration noises estimated for different misregistration values, as we are comparing one image with itself.) To this end, the difference image $\mathbf{X}_d$ is considered, and

the probability $P_l(\mathbf{X}_d)$ that a pixel of the difference image may be contained in the cell s_l is estimated by the following equation:

$$P_l(\mathbf{X}_d) = \frac{g_l(\mathbf{X}_d)}{W \times H} \tag{5}$$

where $g_l(\mathbf{X}_d)$ is the number of difference vectors in the cell s_l. Then, the correlation $R_{x,n}(x_p, y_q)$ between the quantized representation of the global distribution of the difference vectors $p(\mathbf{X}_d)$ and each conditional registration-noise density distribution $p(n/x_p, y_q)$ is computed as follows:

$$R_{x,n}(x_p, y_q) = \frac{1}{N \times L} \cdot \frac{\sum_{i=1}^{N \times L} [P_i(x) - \mu_x][P_i(n/x_p, y_q) - \mu_{n,x_p,y_q}]}{\sqrt{\sigma_x^2 \sigma_{n,x_p,y_q}^2}} \tag{6}$$

where $\mu_x, \mu_{n,x_p,y_q}, \sigma_x^2$, and σ_{n,x_p,y_q}^2 are the mean values and the variances of $P_l(\mathbf{X}_d)$ and $P_l(n/x_p, y_q)$, respectively, for the $N \times L$ quantization cells. The pair of misregistration values $(\hat{x}_p^*, \hat{y}_q^*)$ that maximizes the correlation function $R_{x,n}(x_p, y_q)$ is considered as an estimate of the true (x_p^*, y_q^*), i.e.,

$$(\hat{x}_p^*, \hat{y}_q^*) = \arg \max_{(x_p, y_q) \in \Phi} \{R_{x,n}(x_p, y_q)\}. \tag{7}$$

Consequently, we can write

$$\hat{P}_l(n) = P_l(n/\hat{x}_p^*, \hat{y}_q^*). \tag{8}$$

B. Decision Strategy for Producing the Change-Detection Map

Let us now focus our attention on the distribution $p(\mathbf{X}_d)$ of the difference vectors making up the difference image $\mathbf{X}_d$ in the M–D space. This distribution can be analyzed by comparing it with the registration-noise distribution estimated in the previous phase. The analysis is carried out separately for each quantization cell. From the knowledge of $\hat{P}_l(n)$, it is possible to derive a local decision strategy that allows one to detect changed areas by taking into account the registration noise. (The term "local" refers to the fact that the decision strategy can cope with the different characteristics of the registration noise in the different cells of the M–D space.) Let us consider a generic pixel $x(i,j)$ in the difference image, and let us assume that the difference vector $\mathbf{x}_d(i,j)$ of the pixel lies in the cell s_l. The pixel is associated with changed or unchanged areas according to the decision rule as in (9) (shown at the bottom of the page), where $\varepsilon \in [0,1]$ is a parameter that tunes the tolerance to registration noise. As compared with the standard CVA technique (according to which only the magnitude of the difference vector is usually considered to make the final decision), the decision rule (9) also analyzes the probability that the difference vector considered may be related to registration noise. If the probability of having registration noise is high as compared to the probability of having difference vectors in a given cell for the specific images considered, the corresponding pixel is considered to be affected by registration noise and is labeled as unchanged. The threshold ν_{th} and the parameter ε can be jointly optimized in order to obtain a specific tradeoff between false and missed alarms. It is worth noting that the ability of the proposed approach to explicitly deal with the effects of registration noise (which usually involve large number of false alarms) allows the optimal decision threshold ν_{th} (i.e., the threshold that minimizes the overall change-detection error) to be lower than the threshold used by the standard CVA technique. This may also result in a decrease in the number of missed alarms, as compared with the CVA technique.

The uniform quantization adopted for the M–D space may affect the results of the proposed technique. This is due to the fact that a small amount of noise affecting a difference vector may make it move from one cell to another. In order to reduce the effects of this phenomenon, one can use strategies capable of exploiting the contextual information contained in neighboring quantization cells in the M–D space. In the next section, a simple and effective strategy that can cope with this issue is described.

IV. Contextual Analysis of the M–D Space

As pointed out in the previous section, the uniform quantization adopted for the M–D space may decrease the effectiveness of the proposed technique. In order to mitigate this drawback, in the following a simple strategy is described that exploits the contextual information contained in neighboring quantization cells in the M–D space. The basic idea of this strategy is to analyze the contextual information whenever an ambiguous situation is detected, i.e., the value of the probability $P_l(\mathbf{X}_d)$ is close to the value of the probability $\hat{P}_l(n)$. The contextual information is exploited by merging pairs of neighboring cells and estimating the probabilities of having both registration noise and difference vectors (derived from the analysis of multitemporal images) in these new "macrocells." In greater detail, the decision rule (9) can be rewritten as in (10) (shown at the bottom of the next page), where ε_{low} and ε_{up} (with $\varepsilon_{\text{low}} < \varepsilon_{\text{up}}$ and $\varepsilon_{\text{low}}, \varepsilon_{\text{up}} \in [0,1]$) are two parameters that identify critical uncertainty situations in which the values $P_l(\mathbf{X}_d)$ and $P_l(n)$ are very close to each other, and hence (9) is not appropriate to a reliable final decision. In the case of uncertainty, the cell s_l and its eight neighboring cells are considered (instead of the single cell s_l) and eight macrocells are derived, as shown in Fig. 3. Let $Z_l = \{z_{l,1}, \ldots, z_{l,8}\}$ be the set of macrocells obtained by this strategy. It is worth noting that the original cell s_l is included in each one of the macrocells $Z_l = \{z_{l,1}, \ldots, z_{l,8}\}$. The probability $\hat{P}_l^{z_h}(n)(h = 1, \ldots, 8)$ of having registration noise and the probability $P_l^{z_h}(\mathbf{X}_d)$ of having difference vectors in each

$$x(i,j) \in \begin{cases} \text{change} & \text{if } \left\{x_d^{\text{mag}}(i,j) \geq \nu_{\text{th}} \text{ and } [P_l(\mathbf{X}_d) \geq \hat{P}_l(n) + \varepsilon]\right\} \\ \text{no change} & \text{if } \left\{x_d^{\text{mag}}(i,j) < \nu_{\text{th}} \text{ or } [P_l(\mathbf{X}_d) < \hat{P}_l(n) + \varepsilon]\right\} \end{cases} \tag{9}$$

one of the macrocells $z_{l,h}$ are estimated. For each macrocell $z_{l,h}$ contained in Z_l, the decision rule (11) (shown at the bottom of the page) is used, where the parameter $\varepsilon_{\text{context}} \in [0,1]$ tunes the tolerance to registration noise in the context-based decision. Equation (11) is applied to all the eight macrocells $z_{l,h} \in Z_l$ associated with s_l; then the pixel $x(i,j)$ is labeled as changed or unchanged according to a simple majority rule.

V. Experimental Results

In order to assess the effectiveness of the proposed method, experiments were carried out on two different typologies of remote sensing datasets, i.e., simulated and real multitemporal datasets.

A. Simulated Dataset

The simulated dataset was obtained by the procedure described in the following. A multispectral image acquired by the Daedalus 1268 Airborne Thematic Mapper (ATM) multispectral scanner was used as a reference image. In particular, a section (250×350 pixels) of a scene acquired in an agricultural area near the village of Feltwell, U.K., was selected [see Fig. 4(a)]. (For greater details on this dataset, see [16].) For simplicity, only two spectral channels were considered (i.e., channels 3 and 5 were selected). This image was assumed to be the image $\mathbf{X}_1$ (i.e., the image acquired at time t_1). The image $\mathbf{X}_2$ was obtained by inserting some simulated changes in $\mathbf{X}_1$ [see Fig. 4(b) and (c)]. At this point, the image $\mathbf{X}_2$ was misregistered to the image $\mathbf{X}_1$. In particular, different pairs of simulated multitemporal images with different misregistration values were generated [i.e., (1, 1) (0.5, 1.5) (1.5., 1.5) (1, 2), and (2, 2)]. It is worth noting that these misregistration values are realistic, especially considering that, in real cases, misregistration offsets outside the GCPs may be significantly higher than the ones measured in GCPs themselves.

The standard CVA technique was applied to the different pairs of images generated. A manual trial-and-error procedure was adopted in order to find the optimal threshold $\nu_{\text{th}}^{\text{CVA,opt}}$, i.e., the threshold that minimizes the overall change-detection error. Table I gives the change-detection errors on the different datasets. As one can see, the registration noise affecting the difference image results in a large number of change-detection errors (in particular, a large number of false alarms).

At this point, the proposed technique was applied to the images $\mathbf{X}_1$ and $\mathbf{X}_2$ of the considered simulated datasets (also in this case, different experiments were carried out for the different misregistration values considered). As described in the methodological part, the first step in the proposed approach consists in estimating the distribution of registration noise in the M–D space. In the set Φ, we considered different misregistration values (x_p, y_q), with x_p and y_q ranging from -2 to $+2$ (by a step of 0.25 pixels). The performances of all the estimation strategies (i.e., the mean-based, maximum-based, and correlation-based strategies) were evaluated. Several trials were carried out by using different values of the parameters required by the proposed approach. In particular, the tolerance parameters $\varepsilon, \varepsilon_{\text{low}}, \varepsilon_{\text{up}}$ ranged in $[0, 10^{-4}]$ (under the obvious constraint $\varepsilon_{\text{low}} < \varepsilon_{\text{up}}$); the parameter $\varepsilon_{\text{context}}$ was set equal to the mean of the interval $[\varepsilon_{\text{low}}, \varepsilon_{\text{up}}]$. Concerning the size of the quantization cells, it should be chosen on the basis of the specific dataset analyzed by considering the dimensions of the images and the structure of the scene. On the one hand, this size should be selected sufficiently small to have a precise quantization of the M–D space. On the other hand, it should be sufficiently large to estimate the probabilities in a reliable way. In our experiments, according to the results of a preliminary analysis, the dimensions Δ_M and Δ_D of the quantization cells ranged from 40 to 120 and from 40 to 60, respectively. The best results obtained by the proposed method are given in Table II(a) and (b). In particular, these tables show the results obtained by optimizing the parameters required by the proposed approach according to two different criteria. The results presented in Table II(a) were obtained according to the first criterion, i.e., by optimizing the parameters so that the overall change-detection error was minimized. Table II(b) gives the results yielded by the second criterion, i.e., optimizing the parameters according to a different tradeoff between false and missed alarms. In greater detail, in the latter case, the parameters were selected in order to decrease both missed and false alarms (with respect to the case of the standard CVA technique) and not to minimize the overall change-detection error. All the proposed strategies resulted in significant reductions in false alarms, as respect to the standard CVA. For example, in the case where the parameters were optimized to minimize the total change-detection error, the 632 false alarms incurred by the CVA in the dataset generated by a misalignment of (2, 2) pixels were reduced to 316, 372, and 347 false alarms by the proposed maximum-based, mean-based, and cor-

$$x(i,j) \in \begin{cases} \text{change} & \text{if } \left\{ x_d^{\text{mag}}(i,j) \geq \nu_{\text{th}} \text{ and } [P_l(\mathbf{X}_d) \geq \hat{P}_l(n) + \varepsilon_{\text{up}}] \right\} \\ \text{no change} & \text{if } \left\{ x_d^{\text{mag}}(i,j) < \nu_{\text{th}} \text{ or } [P_l(\mathbf{X}_d) < \hat{P}_l(n) + \varepsilon_{\text{low}}] \right\} \end{cases} \tag{10}$$

$$x(i,j) \in \begin{cases} \text{change} & \text{if } \left\{ x_d^{\text{mag}}(i,j) \geq \nu_{\text{th}} \text{ and } \left[P_l^{z_h}(\mathbf{X}_d) \geq \hat{P}_l^{z_h}(n) + \varepsilon_{\text{context}} \right] \right\} \\ \text{no change} & \text{if } \left\{ x_d^{\text{mag}}(i,j) < \nu_{\text{th}} \text{ or } \left[P_l^{z_h}(\mathbf{X}_d) < \hat{P}_l^{z_h}(n) + \varepsilon_{\text{context}} \right] \right\} \end{cases} \tag{11}$$

TABLE II
BEST CHANGE-DETECTION RESULTS PROVIDED BY THE PROPOSED TECHNIQUE ON THE DIFFERENT SIMULATED DATASETS CONSIDERED. (a) MINIMUM-ERROR CASE. (b) EXAMPLE OF A DIFFERENT TRADEOFF BETWEEN FALSE AND MISSED ALARMS

Misalignment between the simulated multitemporal images	Adopted strategy	Change-detection errors (# pixels)		
		Missed alarms	False alarms	Total error
(2,2)	maximum	191	316	507
	mean	218	372	590
	correlation	227	347	574
(1,2)	maximum	268	171	439
	mean	263	251	514
	correlation	232	269	501
(1.5,1.5)	maximum	155	162	317
	mean	146	238	384
	correlation	156	230	386
(0.5,1.5)	maximum	250	101	351
	mean	224	153	377
	correlation	225	128	353
(1,1)	maximum	255	202	457
	mean	275	232	507
	correlation	275	232	507

(a)

Misalignment between the simulated multitemporal images	Adopted strategy	Change-detection errors (# pixels)		
		Missed alarms	False alarms	Total error
(2,2)	maximum	162	384	546
	mean	157	438	595
	correlation	161	416	577
(1,2)	maximum	213	249	462
	mean	210	313	523
	correlation	232	269	501
(1.5,1.5)	maximum	155	162	317
	mean	146	238	384
	correlation	156	230	386
(0.5,1.5)	maximum	158	244	402
	mean	176	293	469
	correlation	169	270	439
(1,1)	maximum	255	202	457
	mean	275	232	507
	correlation	275	232	507

(b)

relation-based strategies, respectively. Furthermore, when a different tradeoff between false and missed alarms was considered [see Table II(b)], reductions in the numbers of missed alarms were also observed. This is a consequence of the possibility of adopting a threshold $\nu_{\rm th}$ lower than the optimal CVA threshold $\nu_{\rm th}^{\rm CVA,opt}$ resulting from the reduction in the false alarms induced by registration noise. A comparison of the different typologies of errors incurred by the different strategies shows that, as expected, the maximum-based strategy turns out to be the most effective in reducing false alarms. This strategy was also the most effective in obtaining a good trade-off between false and missed alarms (both decreased, as compared with the CVA technique).

In order to assess the robustness of the proposed approach, the means and the standard deviations of the change-detection errors incurred by the three proposed strategies in the different trials with different values of the required parameters (i.e., the dimensions Δ_M and Δ_D of the quantized cells, and the tolerance parameters) were evaluated. The results obtained by both considering and not considering the contextual information in the quantized M–D space are given in Table III(a) and (b), respectively. By analyzing the average values, it is possible to observe that, also in this case, all the proposed strategies resulted in reductions in false alarms, as compared with the standard CVA. Concerning the robustness of the proposed approach, a comparison of the results given in Table III(a) and (b) points out that the contextual analysis of the M–D space: 1) generally results in a slight increase in the average change-detection accuracy; 2) exhibits a significantly stabler behavior versus the choice of the different values of the parameters required by the proposed approach.

Fig. 5(a) and (b) shows the best change-detection maps (i.e., the ones that minimize the total change-detection errors) obtained by the standard CVA technique and the proposed approach with the maximum strategy, respectively, for the dataset generated by a misalignment of (2, 2) pixels (where the effects of the misalignment are more evident). A qualitative analysis of such figures confirms the effectiveness of the proposed approach in sharply reducing the effects of registration noise, as compared with the CVA technique. This is particularly evident at the field boundaries. In addition, it can be observed that, even though a portion of the changed field in the upper right corner

TABLE III
AVERAGE CHANGE-DETECTION ERRORS PROVIDED BY THE PROPOSED TECHNIQUES ON THE DIFFERENT SIMULATED DATASET CONSIDERED. (a) STANDARD ANALYSIS OF THE QUANTIZED M–D SPACE. (b) CONTEXTUAL ANALYSIS OF THE QUANTIZED M–D SPACE

Misalignment between the simulated multitemporal images	Adopted strategy	Change-detection errors (# pixels)					
		Missed alarms		False alarms		Total error	
		mean	stdev	mean	stdev	mean	stdev
(2,2)	maximum	147	43.4	517	124.6	664	86.2
	mean	131	30.7	621	116.7	752	89.9
	correlation	133	32.8	607	117.7	741	89.2
(1,2)	maximum	238	165.6	365	189.7	602	152.2
	mean	223	165.1	467	210.4	690	161.5
	correlation	223	165.1	448	209.3	671	164.2
(1.5,1.5)	maximum	187	57.3	200	83.9	387	40.1
	mean	164	46.0	316	93.3	481	54.4
	correlation	167	46.0	308	92.9	476	53.7
(0.5,1.5)	maximum	221	57.4	196	91.9	417	44.2
	mean	194	43.4	314	135.0	508	99.4
	correlation	196	43.1	288	136.5	484	102.5
(1,1)	maximum	282	43.0	250	56.7	531	32.7
	mean	269	36.5	323	74.7	592	49.5
	correlation	270	36.8	317	71.7	587	45.5

(a)

Misalignment between the simulated multitemporal images	Adopted strategy	Change-detection errors (# pixels)					
		Missed alarms		False alarms		Total error	
		mean	stdev	mean	stdev	mean	stdev
(2,2)	maximum	136	26.2	536	77.5	673	58.0
	mean	129	24.5	622	85.8	752	66.4
	correlation	129	24.5	609	88.5	738	70.0
(1,2)	maximum	238	131.5	299	95.5	537	98.7
	mean	235	132.4	413	132.1	649	86.2
	correlation	235	132.7	399	130.2	634	82.6
(1.5,1.5)	maximum	167	24.5	170	13.7	337	16.7
	mean	149	23.3	318	35.1	467	17.4
	correlation	151	23.5	317	31.7	469	23.7
(0.5,1.5)	maximum	218	32.4	176	20.2	395	21.4
	mean	184	31.5	319	77.1	503	50.7
	correlation	190	32.8	281	69.0	472	42.8
(1,1)	maximum	271	31.4	236	29.7	507	21.9
	mean	264	32.6	315	43.2	579	20.2
	correlation	264	32.6	314	44.3	578	23.7

(b)

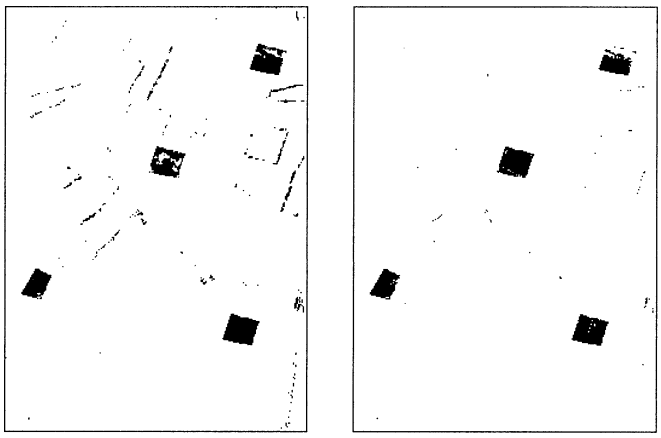

(a) (b)

Fig. 5. Change-detection maps obtained on the simulated dataset generated by a misalignment of (2, 2) pixels by (a) the standard CVA technique and (b) the proposed approach with the maximum strategy.

of the image was not correctly detected, the proposed approach, unlike the standard CVA technique, was able to detect a significant area corresponding to the changed field in the center of the image.

B. Real Dataset

The second dataset consisted of two multispectral images (414×326 pixels) acquired by the Landsat-5 Thematic Mapper (TM) sensor on the Island of Elba, Italy, in August 1992 (image $\mathbf{X}_1$) and September 1994 (image $\mathbf{X}_2$) [see Fig. 6(a) and (b)]. Two wildfires (one occurred in 1993 and the other in 1994) destroyed part of the vegetation between the two acquisition dates. The available ground-truth information about the burnt areas was used to prepare a "reference map" for a quantitative evaluation of the change-detection results [see Fig. 6(c)]. The two images were coregistered using ten GCPs corresponding to points easily recognizable on both images. A root mean square

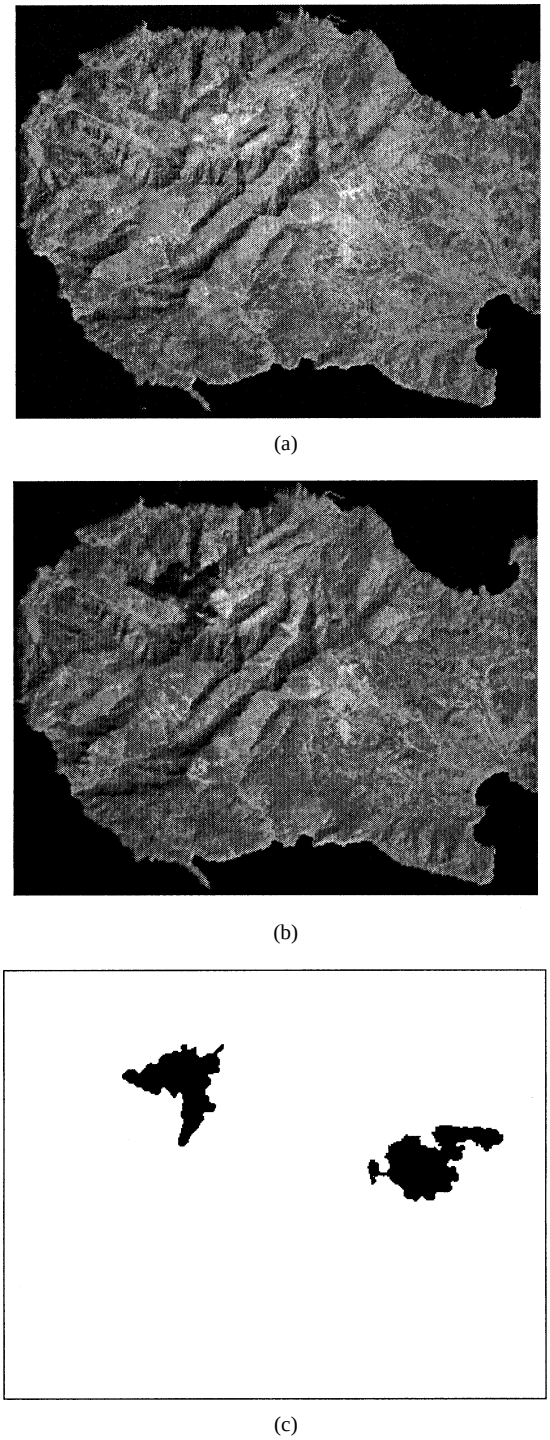

(a) (b) (c)

Fig. 6. Real dataset utilized in the experiments. (a) Channel 4 of the TM image acquired in August 1992. (b) Channel 4 of the TM image acquired in September 1994. (c) Ground-truth map of the changed areas.

error of 0.49 was obtained. It is worth noting that the considered change-detection problem results in a challenging task due to: 1) the presence of registration noise and 2) the fact that the second image was acquired a long time after the 1993 fire event, and consequently, this burnt area is partially covered by the new vegetation that grew in the meanwhile. The standard CVA technique was applied to spectral channels 4 and 7 of the images $\mathbf{X}_1$ and $\mathbf{X}_2$. A manual trial-and-error procedure was adopted to determine the optimal threshold $\nu_{\rm th}^{\rm CVA,opt}$, i.e., the threshold

TABLE IV
CHANGE-DETECTION RESULTS PROVIDED BY THE STANDARD CVA TECHNIQUE ON THE REAL DATASET CONSIDERED

Change-detection errors (# pixels)		
Missed alarms	False alarms	Total error
3256	1340	4596

TABLE V
CHANGE-DETECTION RESULTS PROVIDED BY THE PROPOSED APPROACH ON THE REAL DATASET CONSIDERED (THE ANALYSIS HAS BEEN CARRIED OUT BY CONSIDERING THE CONTEXTUAL INFORMATION IN THE QUANTIZED M–D SPACE)

Adopted strategy	Change-detection errors (# pixels)		
	Missed alarms	False alarms	Total error
Maximum	3197	737	3934
Mean	2979	1087	4066
Correlation	3084	797	3881

that minimizes the overall change-detection error. Table IV gives the change-detection errors incurred with such an optimal threshold. As one can see, the registration noise affecting the difference image induced a large number of change-detection errors (in particular, a large number of false alarms). At this point, the proposed technique was applied. On the basis of the results obtained on the simulated dataset, the analysis of the quantized M–D space was carried out considering the contextual information. The dimensions of the quantization cells, the parameter $\varepsilon_{\rm low}$, and the parameter $\varepsilon_{\rm up}$ were set equal to 40×40, 10^{-7}, and 10^{-4}, respectively. The parameter $\varepsilon_{\rm context}$ was fixed equal to the mean of the interval $[\varepsilon_{\rm low}, \varepsilon_{\rm up}]$. The change-detection errors incurred by the three proposed strategies are presented in Table V. As one can see, also in this case the proposed approach resulted in a significant decrease in the number of change-detection errors (i.e., from 4596 errors incurred by the standard CVA technique to 3934, 4066, and 3881 errors incurred by the maximum-based, mean-based, and correlation-based strategies, respectively). In greater detail, significant reductions were observed both in false alarms (i.e., from 1340 incurred by the standard CVA technique to 737, 1087, and 797 incurred by the maximum-based, mean-based, and correlation-based strategies, respectively) and in missed alarms (i.e., from 3256 incurred by the standard CVA technique to 3197, 2979, and 3084 incurred by the maximum-based, mean-based, and correlation-based strategies, respectively). On the one hand, the decrease in false alarms directly derives from the ability of the proposed approach to cope with the effects of registration noise. On the other hand, the reduction in missed alarms depends on the fact that a threshold lower than the one used for the CVA (i.e., $\nu_{\rm th}^{\rm CVA,opt}$) was adopted. In particular, the optimal threshold $\nu_{\rm th}^{\rm CVA,opt}$ for the standard CVA technique was found to be 44, whereas a threshold $\nu_{\rm th}$ equal to 42 was used for the proposed approach. The analysis of Table V reveals that the maximum-based strategy turned out to be the most effective in reducing false alarms, whereas the correlation-based strategy allowed the best tradeoff between false and missed alarms, thus minimizing the overall change-detection error.

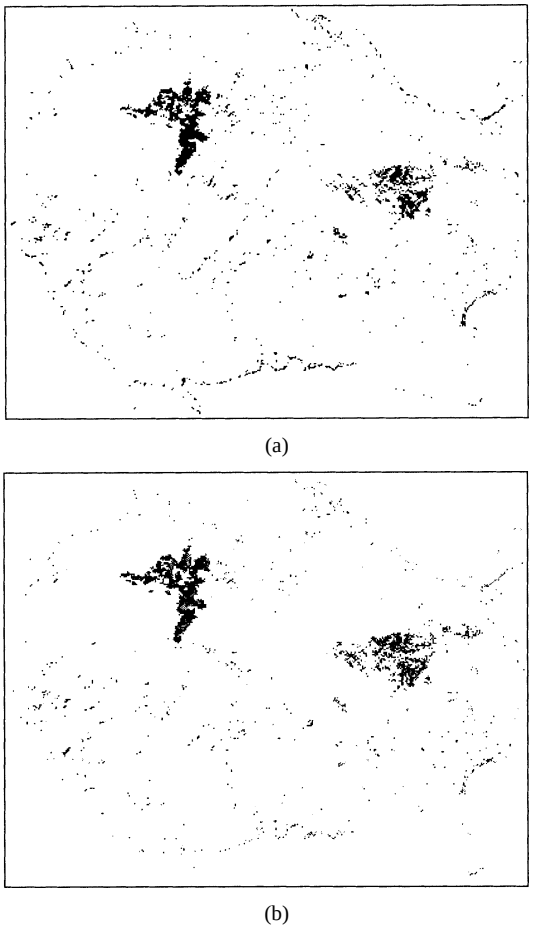

(a)

(b)

Fig. 7. Change-detection maps obtained by (a) the standard CVA technique and (b) the proposed approach with the correlation strategy.

Fig. 7(a) and (b) shows the best change-detection maps obtained by the standard CVA technique and the proposed approach with the correlation strategy, respectively. A qualitative analysis of such maps confirms the effectiveness of the proposed method in sharply reducing the effects of registration noise, as compared with the CVA technique. In particular, the reduction in registration noise is mainly evident along the coastline. In addition, some parts of the eastern burnt area that were missed by the CVA technique were correctly classified by the proposed approach.

It is worth noting that, despite the proposed approach allowing one to significantly decrease the number of false alarms, residual noise still affects the obtained change-detection map. However, in the map produced by the proposed method, noisy pixels are isolated, and consequently, can be easily removed by using standard postprocessing techniques.

VI. Discussion and Conclusion

In this paper, an adaptive approach aimed at reducing the effects of registration noise in unsupervised change detection has been presented. The results of several experiments carried out on both a simulated and a real multitemporal dataset confirm the effectiveness of the described approach, which provided a much higher change-detection accuracy than the standard CVA technique. Such accuracy mainly relies on the ability of the proposed approach to reduce false alarms; however, a reduction in the number of missed alarms was also observed. This is a consequence of the possibility of adopting a threshold $v_{\rm th}$ lower than the optimal CVA threshold $v_{\rm th}^{\rm CVA,opt}$, as one can reduce the effects of registration noise. Three different adaptive strategies have been proposed to estimate the distribution of the registration noise present in the considered multitemporal images. In our experiments, all the strategies allowed us to improve the change-detection accuracy over that of the standard CVA technique. On the one hand, given its properties, the maximum-based strategy is recommended in the cases where false alarms induced by misregistration may be particularly critical to the considered application. On the other hand, the use of the correlation-based strategy is suggested when missed alarms may be serious for the specific problem addressed. Even though, from a general point of view, the proposed approach results in a reduction in the number of missed alarms, as compared with the standard CVA technique, in some experiments, we observed that omission errors may occur in areas where, as opposite, the standard CVA technique performs well (as is the case with the upper-right change polygon in the simulated dataset). In particular, such omission errors are incurred when the difference vector $\boldsymbol{x}_d(i,j)$ of a changed pixel is contained in a cell s_l where the probability of having registration noise is high, as compared with the probability of having difference vectors. Two different reasons can cause such a situation: 1) the quantization of the M–D space is too rough, and consequently, the difference vectors of the changed pixels are compared with registration noise having a significantly different magnitude and direction; 2) registration noise is overestimated. This behavior is more typical for the maximum-based strategy (which, as already observed, may involve an overestimation of registration noise) than for the correlation-based and mean-based strategies.

It is worth noting that, among the aspects that affect registration noise, there are the heterogeneity and homogeneity of the scene under analysis. In the case of scenes composed of different homogeneous areas, registration noise mainly appears along the boundaries of such areas, whereas, in the case of images composed of heterogeneous areas, registration noise has a more spread spatial distribution. Although the proposed approach is intrinsically more suited to being applied to images with homogeneous areas, in most of the experiments we carried out it turned out to be effective also on heterogeneous areas.

Concerning the local decision strategy for deriving the change-detection map, the approach that exploits contextual information in the M–D space proved useful mainly in decreasing the dependence of the change-detection results on the values of the input parameters required by the described method.

Concerning the computation time, the most time-demanding task of the proposed algorithm is the generation of the set of misregistered images (mainly dependent on the application of the DFT transform), the rest of the approach being very fast. However, in operating conditions, the fast Fourier transform (FFT) can be used in place of the DFT, thus reducing the computational complexity.

As future developments of this work, we are exploring the possibilities of: 1) using strategies different from the maximum-

based, mean-based, and correlation-based ones to further increase the accuracy in modeling the registration-noise effects and 2) extending the proposed methodology for estimating the registration-noise distribution in order to deal also with residual rotational effects present in the coregistered images.

As a final remark, it should be stressed that, in this paper, we have focused our attention only on the presence of registration noise. However, as stated in the Introduction, other sources of noise may affect the change-detection process. Therefore, when critical sources of noise are present in the analyzed data, we suggest that the proposed method should be applied together with processing procedures aimed at reducing other undesired noise effects.

ACKNOWLEDGMENT

The authors are grateful to the anonymous referees for their constructive criticism.

REFERENCES

[1] A. Singh, "Digital change detection techniques using remotely-sensed data," *Int. J. Remote Sens.*, vol. 10, pp. 989–1003, 1989.

[2] L. Bruzzone and D. F. Prieto, "Automatic analysis of the difference image for unsupervised change detection," *IEEE Trans. Geosci. Remote Sensing*, vol. 38, pp. 1171–1182, May 2000.

[3] ——, "An adaptive semi-parametric and context-based approach to unsupervised change detection in multitemporal remote sensing images," *IEEE Trans. Image Processing*, vol. 11, pp. 452–466, Apr. 2002.

[4] P. Gong, "Change detection using principal component analysis and fuzzy set theory," *Can. J. Remote Sens.*, vol. 19, no. 1, pp. 22–29, 1993.

[5] X. Dai and S. Khorram, "The effects of image misregistration on the accuracy of remotely sensed change detection," *IEEE Trans. Geosci. Remote Sensing*, vol. 36, pp. 1566–1577, Sept. 1998.

[6] L. M. G. Fonseca and B. S. Manjunath, "Registration techniques for multisensor sensed imagery," *Photogramm. Eng. Remote Sens. J.*, vol. 62, no. 9, pp. 1049–1056, 1996.

[7] A. A. Goshtasby and J. Le Moigne, "Special issue on image registration," *Pattern Recognit.*, vol. 32, no. 1, 1999.

[8] J. Le Moigne, "An automated parallel image registration technique based on the correlation of wavelet features," *IEEE Trans. Geosci. Remote Sensing*, vol. 40, pp. 1849–1864, Aug. 2002.

[9] J. R. G. Townshend, C. O. Justice, and C. Gurney, "The impact of misregistration on change detection," *IEEE Trans. Geosci. Remote Sensing*, vol. 30, pp. 1054–1060, Sept. 1992.

[10] P. Gong, E. F. Ledrew, and J. R. Miller, "Registration-noise reduction in difference images for change detection," *Int. J. Remote Sens.*, vol. 13, no. 4, pp. 773–779, 1992.

[11] L. Bruzzone and S. B. Serpico, "Detection of changes in remotely-sensed images by the selective use of multi-spectral information," *Int. J. Remote Sens.*, vol. 18, no. 18, pp. 3883–3888, 1997.

[12] D. Stow, "Reducing misregistration effects for pixel-level analysis of land-cover change," *Int. J. Remote Sens.*, vol. 20, pp. 2477–2483, 1999.

[13] D. Stow, D. Chen, and L. Coulter, "Detection of pixel-level land-cover changes with multi-temporal imagery: Theory and examples with imagery of 1 meter and 1 kilometer spatial resolutions," in *Analysis of Multi-Temporal Remote Sensing Images*, L. Bruzzone and P. Smits, Eds, Singapore: World Scientific, 2002, pp. 59–66.

[14] J. A. Richards, *Remote Sensing Digital Image Analysis*, 2nd ed. New York: Springer-Verlag, 1993.

[15] R. A. Schowengerdt, *Remote Sensing*, 2nd ed. San Diego, CA: Academic, 1997.

[16] L. Bruzzone and D. F. Prieto, "A technique for the selection of kernel-function parameters in RBF neural networks for classification of remote-sensing images," *IEEE Trans. Geosci. Remote Sensing*, vol. 37, pp. 1179–1184, Mar. 1999.

Lorenzo Bruzzone (S'95–M'99–SM'03) received the laurea (M.S.) degree in electronic engineering (summa cum laude) and the Ph.D. degree in telecommunications, both from the University of Genoa, Genoa, Italy, in 1993 and 1998, respectively.

He is currently Head of the Remote Sensing Laboratory in the Department of Information and Communication Technologies at the University of Trento, Trento, Italy. From 1998 to 2000, he was a Postdoctoral Researcher at the University of Genoa. From 2000 to 2001, he was an Assistant Professor at the University of Trento, where he has been an Associate Professor of telecommunications since November 2001. He currently teaches remote sensing, pattern recognition, and electrical communications. His current research interests are in the area of remote sensing image processing and recognition (analysis of multitemporal data, feature selection, classification, data fusion, and neural networks). He conducts and supervises research on these topics within the frameworks of several national and international projects. He is the author (or coauthor) of more than 90 scientific publications, including journals, book chapters, and conference proceedings. He is a referee for many international journals and has served on the Scientific Committees of several international conferences.

Dr. Bruzzone is the Delegate in the scientific board for the University of Trento of the Italian Consortium for Telecommunications (CNIT). He is a member of the Scientific Committee of the India–Italy Center for Advanced Research. He was the General Co-Chair of the First and Second IEEE International Workshop on the Analysis of Multi-Temporal Remote-Sensing Images (Trento, Italy, September 2001, and Ispra, Italy, July 2003). Since 2003, he has been the Chair of the SPIE Conference on Signal and Image Processing for Remote Sensing (Barcelona, Spain, September 2003 and Maspalomas, Gran Canaria, September 2004). He is a member of the International Association for Pattern Recognition (IAPR) and of the Italian Association for Remote Sensing. He ranked first place in the Student Prize Paper Competition of the 1998 IEEE International Geoscience and Remote Sensing Symposium (Seattle, WA, July 1998) and was a recipient of the *Recognition of IEEE Transactions on Geoscience and Remote Sensing Best Reviewers* in 1999.

Roberto Cossu (S'02) received the laurea (M.S.) degree in electronic engineering (summa cum laude) from the University of Genoa, Genoa, Italy, in 1999. He partially carried out his master's thesis at the Sheffield Centre of Earth Observation Science (S.C.E.O.S), Sheffield University, Sheffield, U.K. He is currently pursuing the Ph.D. degree at the University of Trento, Trento, Italy.

His main research activity is in the area of remote sensing image processing and recognition. In particular, his interests include neural networks for classification purposes, partially unsupervised updating of land-cover maps, and supervised and unsupervised change detection techniques. In these fields, he conducts research within several national and international projects. He is a reviewer for the *Journal of Remote Sensing*.

Mr. Cossu is a reviewer for the IEEE TRANSACTIONS ON GEOSCIENCE AND REMOTE SENSING. He has served on the local committee of the First International Workshop on the Analysis of Multi-Temporal Remote Sensing Images (MultiTemp-2001, Trento, September 2001), and he is a member of the Italian Consortium for Telecommunications (CNIT) and the Italian Elettrotechnical Association (AEI).